

Published in final edited form as:

Birth Defects Res A Clin Mol Teratol. 2010 April ; 88(4): 232–240. doi:10.1002/bdra.20656.

Cleft lip and palate results from Hedgehog signaling antagonism in the mouse: phenotypic characterization and clinical implications

Robert J. Lipinski^{1,2,4,*}, Chihwa Song³, Kathleen K. Sulik⁴, Joshua L. Everson², Jerry J. Gipp², Dong Yan⁴, Wade Bushman^{1,2}, and Ian Rowland⁵

¹ Molecular and Environmental Toxicology Center, School of Medicine and Public Health, University of Wisconsin-Madison, Madison, WI

² Department of Urology, School of Medicine and Public Health, University of Wisconsin-Madison, Madison, WI

³ Department of Medical Physics, School of Medicine and Public Health, University of Wisconsin-Madison, Madison, WI

⁴ Department of Cell and Developmental Biology and The Bowles Center for Alcohol Research, University of North Carolina, Chapel Hill, Chapel Hill, NC

⁵ Department of Radiology, School of Medicine and Public Health, University of Wisconsin-Madison, Madison, WI

Abstract

Background—The Hedgehog (Hh) pathway provides inductive signals critical for developmental patterning of the brain and face. In humans as well as in animal model systems, interference with this pathway yields birth defects; among the most well-studied of which fall within the holoprosencephaly (HPE) spectrum.

Methods—Timed-pregnant C57Bl/6J mice were treated with the natural Hh signaling antagonist cyclopamine by subcutaneous infusion from gestational day (GD) 8.25 to GD 9.5, or with a potent cyclopamine-analog, AZ75, administered by oral gavage at GD 8.5. Subsequent embryonic morphogenesis and fetal CNS phenotype were respectively investigated by scanning electron microscopy and high resolution magnetic resonance imaging (MRI).

Results—*In utero* Hh signaling antagonist exposure induced a spectrum of craniofacial and brain malformations. Cyclopamine exposure caused lateral cleft lip and cleft palate (CLP) defects attributable to embryonic deficiency of midline and lower medial nasal prominence tissue. The CLP phenotype was accompanied by olfactory bulb hypoplasia and anterior pituitary aplasia but otherwise grossly normal brain morphology. AZ75 exposure caused alobar and semilobar HPE with associated median facial deficiencies. An intermediate phenotype of median CLP was produced infrequently by both drug administration regimens.

Conclusions—The results of this study suggest that interference with Hh signaling should be considered in the CLP differential and highlight the occurrence of CNS defects as are expected to be present in a cohort of patients having CLP. This work also illustrates the utility of fetal MRI-based analyses and establishes a novel mouse model for teratogen-induced CLP.

*Correspondence to: Robert Lipinski, University of North Carolina, Rm 3017 Thurston Bowles Bldg, CB# 7178, Chapel Hill, NC 27599. Lipinski@med.unc.edu.

Keywords

cleft lip; cleft palate; holoprosencephaly; hedgehog signaling; cyclopamine

Introduction

Clefts of the lip and/or palate (CL/P) represent the most common birth defect form present in newborns, occurring in approximately 1 in 700 births (reviewed in Vieira, 2008). Of those affected, 20% present with cleft lip (CL), 30% with cleft palate (CP), and 50% with cleft lip and palate (CLP). These defects cause significant morbidity and require extensive medical intervention (reviewed in Robin et al., 2006).

Research efforts to elucidate the etiology of CL/P have largely focused on possible genetic causes. While several allelic variants have been identified that appear to exert predisposing or protective effects, the majority of CL/P cases are considered non-Mendelian. Several environmental factors have been identified that appear to increase the risk of clefting as well, including maternal cigarette smoking, folic acid deficiency, and alcohol consumption (Reviewed in Juriloff and Harris, 2008). However, the currently identified environmental and genetic factors can independently account for only a minority of cases, fueling the hypothesis that the majority of CLP cases have multifactorial etiologies involving the interaction of genetic predisposition with environmental factors and/or teratogenic insults (Murray, 2002; Graham and Shaw, 2007; Vieira, 2008).

In approximately 25% of all cases, clefts of the lip and palate present as part of a more extensive syndrome. An increasing number of genes are being identified as playing a causal role in these syndromic cases. Importantly however, it is clear that even in cases considered nonsyndromic, CL/P preferentially co-occurs with a range of other clinical presentations including congenital heart defects, mild structural brain anomalies, subtle cognitive deficits, and altered pituitary function (Laron and Opitz, 1969; Roitman and Laron, 1978; Rudman et al., 1978; Nopoulos et al., 2002; Swanenburg de Veye et al, 2003; Conrad et al., 2008; Beriaghi et al., 2009).

Of particular significance for this investigation is the association of CL/P with a spectrum of abnormalities termed holoprosencephaly (HPE). Characterized by median forebrain deficiency, HPE typically co-occurs with median facial deficiencies, reduced interocular distance, high arching or clefting of the palate, and median or lateral clefts of the lip (Reviewed in Cohen, 2006 and Dubourg et al., 2007). HPE cases with lateral cleft lip commonly share phenotypic overlap with other named syndromes including Kallmann Syndrome and Oral-Facial-Digital Syndrome. While HPE occurs infrequently in live births (1.3/10,000), its prevalence as well as its prenatal lethality or co-occurrence with lethal birth defects, is illustrated by an incidence in conceptuses of approximately 1 in 250 (Matsunaga and Shiota, 1977; Leoncini et al., 2008).

Human genetic analyses, as well as transgenic and teratogenic animal models, have provided significant insight into the genesis of HPE. While interference with several signaling networks, including Nodal, Wnt, BMP, and Hedgehog (Hh), can yield HPE phenotypes, the latter pathway has been most extensively linked to the genesis of HPE (reviewed in Schachter and Krauss, 2008). *Sonic Hedgehog (Shh)*, encodes a secreted, cholesterol modified ligand that initiates signal transduction, and is expressed in the prechordal plate, ventral forebrain neuroepithelium, ventral facial ectoderm, and palatal oral epithelium (Jeong et al., 2004, Cordero et al., 2004, Rice et al., 2005, Aoto et al., 2008). *Shh* homozygous null mice exhibit severe HPE (Chiang et al., 1996), while heterozygous

hypomorphic mutations in the *Shh* gene are associated with human HPE (Nanni et al., 1999, Maity et al., 2005).

In addition to genetic abrogation, interference with Hh signaling by environmental agents has been informative. The plant alkaloid, cyclopamine, is a specific Hh signaling antagonist that was first shown in the 1960s to cause HPE-associated defects in sheep and has since been employed in teratogenesis studies involving a variety of vertebrates (Keeler, 1978; Omnell et al., 1990; Coventry et al., 1998). Cyclopamine inhibits the morphogenetic activity of the Hh pathway by binding to, and preventing activation of the transmembrane protein Smoothed (Smo) (Chen et al., 2002). In the absence of Hh ligand, its receptor, Patched (Ptc1) inhibits Smo activity, presumptively through a small molecule mediator (Bijlsma et al., 2006; Taipale et al., 2002). Upon Hh binding to Ptc1, inhibition of Smo is relieved, triggering a complex downstream signaling cascade that culminates in target gene activation via the Gli family of transcription factors (reviewed in Ingham and McMahon, 2001).

While Hh signaling perturbation is a well-established mechanism for induction of the concurrent brain and face abnormalities that characterize HPE, recent studies suggest a capacity for induction of facial dysmorphism independent of apparent gross brain defects. In the chick, *Shh* expression in the neuroectoderm is required for induction of Hh signaling in the adjacent face and expansion of the frontonasal prominence (Marcucio et al., 2005). Hh signaling inhibition during neural plate patterning induces severe HPE, while inhibition following establishment of *Shh* in the forebrain but prior to its induction in the face, results in facial defects without apparent effects on the forebrain (Cordero et al., 2004). We have previously demonstrated the induction of CLP in mice by cyclopamine exposure targeting gestational day 8.25 (GD8.25) to GD9.5 (Lipinski et al., 2008a).

For the current investigation, we employed cyclopamine and a potent cyclopamine-analog to examine a phenotypic spectrum resulting from transient *in utero* Hh signaling inhibition in mice. For this work, along with traditional imaging and histological approaches, high resolution magnetic resonance imaging (MRI) was utilized, facilitating the assessment of craniofacial and CNS abnormalities.

Materials and Methods

In vitro cell culture assays

Dose-response assays in Shh LIGHTII NIH3T3 fibroblasts were performed as previously described (Lipinski et al., 2007). Briefly, cells were plated in Multiwell Primaria 24-well plates (Falcon, Franklin Lakes, NJ) at 1.5×10^5 cells/well in 400 μ l media and allowed to attach overnight. Media were then replaced with DMEM containing 1% fetal calf serum (FCS) \pm 1nM octylated human Shh peptide (Curis/Genentech) and cyclopamine (LC Laboratories, Woburn, MA) or AZ75 (Astrazeneca, Waltham, MA) (from 5 mM stock solutions dissolved in 95% ethanol), or vehicle alone. Following 48 hrs incubation, reporter activity was determined by dual luciferase assay (Promega, Madison, WI).

Animals

All animal procedures were conducted in accordance with the University of Wisconsin animal care guidelines. Timed pregnancies were established in-house. Two female C57BL/6J (Jackson Laboratories, Bar Harbor, ME) mice at 12–16 weeks of age were housed with one male C57BL/6J mouse overnight on a light cycle of 12 h on and 12 h off. The presence of a vaginal plug the following morning was considered gestational day 0.5 (GD0.5).

Drug administration

Cyclopamine was administered by subcutaneous infusion via micro-osmotic pump at a rate of 160 mg/kg/d between GD8.25 and GD9.5 as previously described (Lipinski et al., 2008a). AZ75, a synthetic cyclopamine-analog (AstraZeneca, Waltham, MA) was administered at GD8.5 as a single oral gavage dose of 40 or 80 mg/kg in 500 μ l 0.5% hydroxypropyl-methylcellulose (Sigma-Aldrich, St. Louis, MO), 0.1% tween in water.

Specimen preparation

Fetal mice were fixed and stored in 10% formalin indefinitely. For images presented in Figure 1, the fetuses were briefly soaked in ethidium bromide (1 μ g/ml PBS) and imaged under ultraviolet light. For MRI analysis, the specimens were dehydrated in a 4% saline solution for 24 h, and subsequently allowed to rehydrate in 5 mM Multihance[®] (Bracco Diagnostics Inc., Princeton, NJ) (1:99 dilution with 0.9% saline) solution for at least 10 days prior to imaging.

Magnetic Resonance Imaging

Multihance[®]-soaked fetuses were placed into a syringe containing Fluorinert (3M, St. Paul, MN) and positioned centrally in a Varian n.m cm diameter quadrature coil. Images were acquired at 4.7T using a Varian Inova imaging and spectroscopy system. A 3D gradient echo sequence (Tr=20ms, Te=6.5 ms, Fl=65, FOV= 24 \times 12 \times 12mm, Ma=512 \times 256 \times 256, NT=32) was used to acquire images with an isotropic resolution of approximately 47 μ m.

Image construction

ImageJ (Abramoff, 2004) was used to construct 2D images and produce linear measurements (Figures 4 and 5). 3D volume and surface renderings (Figure 4) were obtained using Osirix4 (Rosset et al., 2004). Brain segmentation (Figure 5) was performed using Amira[®] (version 4.1.1, Visage Imaging, Inc., San Diego, USA.).

Histology

Fetuses were fixed in Bouin's solution (Sigma-Aldrich) for at least one week and then transferred to 70% ethanol. Following paraffin embedding, 10 μ m sections were produced and stained with hematoxylin and eosin by standard protocols.

Scanning Electron Microscopy

Embryos at indicated stages were fixed in 2.5% glutaraldehyde in Sorenson's buffer and imaged by light microscopy. Specimens were then processed for imaging by scanning electron microscopy as previously described (Dunty et al., 2002).

Statistical analysis

Linear and volumetric brain measurements were determined for the following sample sizes for each group: Normal, n=4; CLP, n=6; HPE, n=6. Values shown represent mean \pm standard deviation. One way analyses of variance (ANOVA) were utilized to assess differences in measurements among groups. Dunnett post hoc tests were used to follow-up significant results, comparing CLP and HPE groups against the normal group. An alpha-value of 0.05 was maintained for all analyses.

Results

Cyclopamine was administered by subcutaneous infusion that extended from days 8.25 to 9.5 of pregnancy, representing a maternal dosage of 160 mg/kg/d. Cyclopamine exposure

induced gross facial malformations in 5 of 14 litters with an approximate intra-litter penetrance of 50%. One affected fetus exhibited unilateral CL while the majority presented with unilateral (n=6) or bilateral CLP (n=12) as previously reported (Lipinski et al., 2008a; Figure 1). Of the 18 fetuses featuring CLP, the medial nasal prominence-derived tissue mass was markedly deficient in two (Figure 2C), and nearly absent in one (Figure 2D). The varying facial morphologies present in these cycloamine-exposed fetuses are comparable to those occurring in human populations.

AZ75, a semi-synthetic cycloamine-analog, demonstrated a four-fold greater potency for Hh signaling inhibition than its parent compound cycloamine in a ligand-responsive cell line (supplemental Figure 1), with differences also notable *in vivo*. Whereas bolus administration of cycloamine has been associated with maternal toxicity (Lipinski et al., 2008a), administration of AZ75 by oral gavage at doses of 40 mg/kg (n=7) and 80 mg/kg (n=4) on day 8.5 of pregnancy produced no apparent toxicity in the dams. In exposed litters, the 80 mg/kg dose caused all of the embryos to resorb. In the 40 mg/kg exposure group, multiple surviving fetuses were found, with gross craniofacial malformations occurring in 6 of 7 litters.

Regarding craniofacial defects, AZ75 administered acutely by oral gavage on day 8.5 of pregnancy resulted in abnormalities that are consistent with overt (alobar and semilobar) HPE. Among six affected litters, approximately 40% of fetuses exhibited hypotelorism (reduced interocular distance) and cebocephaly (small nose with a single nostril) (Figure 1D,E). In one litter, along with two fetuses exhibiting this phenotype, two littermates presented with median CLP with an almost complete absence of medial nasal prominence-derived tissue (Figure 1C).

To investigate the morphogenesis of cycloamine-induced CLP, embryos were analyzed at GD11.25, the gestational period closely following that in which the medial nasal, lateral nasal, and maxillary prominences unite to form the upper lip (Reviewed by Jiang et al., 2006; Figure 2). Cycloamine-affected embryos presented with medial nasal prominences that were too closely situated and for which the lower component – that from which the philtrum and primary palate are derived – was reduced in size and failed to contact both the maxillary and the lateral nasal prominences. Embryos were also analyzed at GD14.0, a time when the maxillary prominence-derived secondary palatal shelves normally begin to elevate to allow midline approximation and fusion. In embryos with cycloamine-induced CL, the secondary palatal shelves appeared to be of normal size and conformation. However, the midface of affected embryos was slightly wider than normal (compare Fig. 2H and K), with the anterior aspect of the palatal shelves being too widely spaced (compare Fig. 2I and L). In severely holoprosencephalic embryos, where the midface is extremely narrow and the primary palate is absent, the secondary palatal shelves were of relatively normal proportion and were prematurely fused anteriorly.

For further detailed analysis, histological sections were produced from GD16.5 fetuses selected by external appearance to represent the predominant phenotype associated with exposure to vehicle (normal), cycloamine (unilateral and bilateral CLP as depicted in Figure 1F and G), and AZ75 (HPE of severity within the range seen in Figure 1D and E). In the CLP group, both palatal shelves appeared properly elevated in one fetus, whereas in the other three examined, one shelf was elevated while the contralateral was not (Figure 3). Additionally, three of the four CLP specimens exhibited agenesis of the Rathke's pouch-derived anterior lobe of the pituitary gland. For the HPE group, histological sections illustrated that the median facial deficiency reflected that in the forebrain. Olfactory bulb agenesis, rostrally unified cerebral hemispheres (with striatal union), and complete agenesis of the pituitary gland were observed. Additionally, palatal shelves were found to be fused

but abnormally highly arched. No apparent changes in histological features of the midbrain and hindbrain were observed in either group.

From selected fetuses, 48 μm isotropic MRI sections were reconstructed to provide 3-D visualization of skeletal structure and brain surface morphology. Images representing Normal, CLP, and HPE phenotypes are shown in Figure 4. While the CLP-associated craniofacial skeletal structure was grossly normal, abnormal fusion of the frontal bones (metopic craniosynostosis) was associated with the HPE phenotype, reflecting clinical observations (Faro et al., 2005).

To quantitatively assess the CLP- and HPE-associated CNS phenotype, a series of linear measurements was employed (adapted from Parnell et al. 2009). Mid-sagittal brain length, biparietal diameter, transverse cerebellar distance, olfactory bulb length and width, and interocular distance measurements were produced. Figure 5 illustrates linear measurement parameters with corresponding quantitative graphical analysis. This analysis revealed a significant reduction in olfactory bulb length ($F(2, 13) = 592.1, p < 0.001$) and width ($F(2, 13) = 473.4, p < 0.001$) associated with CLP. Holoprosencephalic fetuses exhibited reduced biparietal diameter ($F(2, 13) = 13.5, p < 0.02$) and brain length ($F(2, 13) = 10.9, p < 0.03$), olfactory bulb absence, and severely reduced inter-ocular distance ($F(2, 13) = 17.1, p < 0.001$). Cerebellum width in HPE fetuses was not significantly reduced ($F(2, 13) = 3.7, p < 0.08$).

Segmentation and 3-D reconstruction was used to examine brain morphology associated with the described CLP and HPE phenotypes (Figure 5). As predicted from linear measurements, a subtle but consistent hypoplasia of the olfactory bulbs was observed in brains of mice with cycloamine-induced CLP. No other gross morphological differences in these brains were observed. As expected, striking forebrain abnormalities were observed in the holoprosencephalic fetuses; most notably, median union of the cerebral hemispheres accompanied by rostral-caudal foreshortening. While overall brain volume was unchanged in the CLP group, it was significantly reduced in the HPE group ($F(2, 13) = 13.6, p < 0.001$).

Discussion

Since the first description of cycloamine-mediated teratogenicity, over 40 years ago, the majority of teratology investigations regarding this compound have been directed toward exploring the pathogenesis and mechanisms underlying HPE. This work has led to the appreciation of cycloamine as a Hh antagonist and helped to clarify the role of Hh signaling in normal and abnormal development. Extending this line of investigation is the work described herein, providing new insights into cycloamine-induced CNS and facial defects, and highlighting lateral cleft lip and palate as a manifestation of interference with the Hh pathway. As indicated in a recent review (Gritli-Linde, 2008), our understanding of the genesis of CLP has suffered from the relative infrequency of genetic and teratogen-mediated CLP models. The mouse model established in this investigation holds significant promise in this regard.

This study showed that among the fetuses presenting with lateral CLP, the facial morphology varied. In some fetuses, the medial nasal prominence tissue was clearly deficient in size and in others it was not. For the latter group, the clefts appear comparable to those in clinical populations with “typical” cleft lip. The accompanying anterior pituitary and olfactory bulb deficiencies in this group of animals, however, place the dysmorphology within the HPE spectrum. This is important clinically. Several studies have described an association between nonsyndromic CL/P and reduced body size attributable, at least in part, to anterior pituitary dysfunction (Laron and Opitz, 1969; Roitman and Laron; 1978, Rudman

et al., 1978; Bowers et al., 1987). The findings of the study by Rudman et al. (1978) examining stature and endocrine function in a large clinical sample size suggested that children with CL/P defects have short stature about four times more often, and growth hormone-deficiency about 40 times more often, than children without CL/P. Additionally, Richman et al., (1988) described a significant olfactory deficit in boys with CL/P. This, along with increasing evidence of additional concurrent subtle brain malformations in CL/P patients (Nopoulos et al., 2002, Nopoulos et al., 2007) strongly argues for increased clinical attention to CNS abnormalities that may not be readily detectable and for additional CNS analyses in CLP models.

Our analysis of cyclopamine-exposed embryos suggests that the described fetal phenotype of anterior pituitary aplasia results from embryonic midline tissue deficiency. In these animals, abnormal median approximation of the medial nasal prominences corresponds with a deficient median aspect of the oral cavity, from which Rathke's pouch evaginates. In addition to median approximation, abnormal size and angle of the lower component of the medial nasal prominences in affected embryos appears to be the basis for cyclopamine-induced CL. That the secondary palatal shelves of cyclopamine-exposed embryos did not appear deficient in size argues that the subsequent secondary palate cleft is not due to a direct effect on growth of the maxillary prominence-derived shelves. Rather, we speculate that a subtle increase in midface width, secondary to cyclopamine-induced CL, precludes contact of the palatal shelves at the midline. Excessive midface width as a basis for CP secondary to CL has been extensively proposed for both animal models and clinical populations (Subtelny, 1955; Huddart et al., 1969; Smiley, 1971; Diewert, 1982)

As evidenced by the induction of an intermediate phenotype of median CLP (compare Fig. 1C and I), the two distinct drug administration regimens employed here produced a phenotypic spectrum. We expect that differences in timing of exposure and/or potency of the mechanistically identical drugs are responsible for their preferential induction of distinct phenotypic forms. Elucidation of these factors may provide significant insight into the dynamic role of Hh signaling in craniofacial and CNS development as well as distinct phenotypes within the clinical spectrum of CLP and HPE, and will be the focus of future studies.

As shown herein, for both CNS and craniofacial morphological analyses, MRI provides numerous advantages over traditional histological approaches. This includes generation of virtual 2-D sections in any plane, 3-D segment reconstruction, and acquisition of precise linear and volumetric measurements of specific structures of interest. This study expands upon a body of work illustrating the utility of MR-based fetal phenotypic assessment by describing a novel specimen preparation and imaging methodology. While this protocol does not replicate the contrast and resolution of that reported by Schneider et al., (2004) and Petiet et al., (2008) respectively using 11.9 and 9.0 T magnets, it does produce 48 μm isotropic resolution images allowing visualization and quantitation of gross fetal craniofacial structures. This methodology also provides significant advantages as it is compatible with post-fixation specimens, uses a more commonly available 4.7T magnet, and yields remarkably accurate and detailed 3-D visualization of both soft and hard tissue structures.

Previous studies have shown that a number of different teratogens can induce HPE. This includes acute exposure to retinoic acid, ethanol, and cholesterol biosynthesis inhibitors (Sulik and Johnston 1983; Sulik et al., 1995; Incardona and Roelink, 2000). For at least the latter two, interference with Hh signaling, appears to account for the induced defects (Incardona and Roelink, 2000; Ahlgren et al., 2002; Li et al., 2007). Additionally, a surprising number of structurally diverse synthetic and natural compounds have been identified that act as direct Hh pathway inhibitors (Frank-Kamenetsky et al., 2002; Williams

et al. 2003; Lipinski et al., 2007; Lauth et al., 2007). Efforts to better understand how these agents may act in additive or synergistic fashions, as well as how normally silent genetic mutations may alter sensitivity to such chemical insults should be pursued. Indeed, the fidelity of craniofacial development between man and mouse (Diewert and Wang, 1992) and the unmatched genetic manipulability of the latter, make the mouse an ideal model system in which to investigate the interaction of chemical and genetic factors in the etiopathology of complex birth defects such as CLP and HPE.

Supplementary Material

Refer to Web version on PubMed Central for supplementary material.

Acknowledgments

The authors are deeply grateful to AstraZeneca for sharing AZ75. We wish to thank Deborah Dehart for valuable technical assistance, Dr. Ida Washington for critical review of the manuscript, and Dr. Shonagh O'Leary-Moore for assistance with statistical analyses. This work was supported by grants from National Institutes of Health (DK065303-03); National Institute of Environmental Health Sciences (T32-ES007015); National Institutes of Health (DK056238); National Institutes of Health (AA11605); National Institutes of Health (AA017124); University of Wisconsin-Madison, Department of Surgery, Division of Plastic Surgery.

References

- Abramoff MD, Magelhaes PJ, Ram SJ. Image Processing with Image. *J Biophotonics International* 2004;11:36–42.
- Ahlgren SC, Thakur V, Bronner-Fraser M. Sonic hedgehog rescues cranial neural crest from cell death induced by ethanol exposure. *Proc Natl Acad Sci U S A* 2002;99:10476–81. [PubMed: 12140368]
- Aoto K, Shikata V, Imai H, Matsumara D, Tokunaga T, Shioda S, Yamada G, Motoyama J. Mouse Shh is required for prechordal plate maintenance during brain and craniofacial morphogenesis. *Dev Dio* 2009;327:106–20.
- Beriaghi S, Myers SL, Jensen SA, Kaimal S, Chan CM, Schaefer GB. Cleft lip and palate: association with other congenital malformations. *J Clin Pediatr Dent* 2009;33:207–10. [PubMed: 19476092]
- Bijlsma MF, Spek CA, Zivkovic D, van de Water S, Rezaee F, Peppelenbosch MP. Repression of smoothed by patched-dependent (pro-)vitamin D3 secretion. *PLoS Biol* 2006;4:e232. [PubMed: 16895439]
- Chen JK, Taipale J, Cooper MK, Beachy PA. Inhibition of Hedgehog signaling by direct binding of cyclopamine to Smoothed. *Genes Dev* 2002;16:2743–8. [PubMed: 12414725]
- Cohen MM Jr. Holoprosencephaly: clinical, anatomic, and molecular dimensions. *Birth Defects Res A Clin Mol Teratol* 2006;76:658–73. [PubMed: 17001700]
- Conrad AL, Canady J, Richman L, Nopoulos P. Incidence of neurological soft signs in children with isolated cleft of the lip or palate. *Percept Mot Skills* 2008;106:197–206. [PubMed: 18459368]
- Cordero D, Marcucio R, Hu D, Gaffield W, Tapadia M, Helms JA. Temporal perturbations in sonic hedgehog signaling elicit the spectrum of holoprosencephaly phenotypes. *J Clin Invest* 2004;114:485–94. [PubMed: 15314685]
- Coventry S, Kapur RP, Siebert JR. Cyclopamine-induced holoprosencephaly and associated craniofacial malformations in the golden hamster: anatomic and molecular events. *Pediatr Dev Pathol* 1998;1:29–41. [PubMed: 10463269]
- Diewert VM. A comparative study of craniofacial growth during secondary palate development in four strains of mice. *J Craniofac Genet Dev Biol* 1982;2:247–263. [PubMed: 7183704]
- Diewert VM, Wang KY. Recent advances in primary palate and midface morphogenesis research. *Crit Rev Oral Biol Med* 1992;4:111–30. [PubMed: 1457684]
- Dubourg C, Bendavid C, Pasquier L, Henry C, Odent S, David V. Holoprosencephaly. *Orphanet J Rare Dis* 2007;2:8. [PubMed: 17274816]
- Dunty WC Jr, Zucker RM, Suli KK. Hindbrain and cranial nerve dysmorphogenesis result from acute maternal ethanol administration. *Dev Neurosci* 2002;24:328–42. [PubMed: 12457071]

- Faro C, Wegrzyn P, Benoit B, Chaoui R, Nicolaides KH. Metopic suture in fetuses with holoprosencephaly at 11 + 0 to 13 + 6 weeks of gestation. *Ultrasound Obstet Gynecol* 2006;27:162–6. [PubMed: 16285016]
- Fechner A, Fong S, McGovern P. A review of Kallmann syndrome: genetics, pathophysiology, and clinical management. *Obstet Gynecol Surv* 2008;63:189–94. [PubMed: 18279545]
- Frank-Kamenetsky M, Zhang XM, Bottega S, Guicherit O, Wichterle H, Dudek H, Bumcrot D, Wang FY, Jones S, Shulok J, Rubin LL, Porter JA. Small-molecule modulators of Hedgehog signaling: identification and characterization of Smoothed agonists and antagonists. *J Biol* 2002;1:10. [PubMed: 12437772]
- Graham JM Jr, Shaw GM. Gene-environment interactions in rare diseases that include common birth defects. *Birth Defects Res A Clin Mol Teratol* 2005;73:865–7. [PubMed: 16265646]
- Gritli-Linde A. The etiopathogenesis of cleft lip and cleft palate: usefulness and caveats of mouse models. *Curr Top Dev Biol* 2008;84:37–138. [PubMed: 19186243]
- Huddart AG, MacCauley FJ, Davis ME. Maxillary arch dimensions in normal and unilateral cleft palate subjects. *Cleft Palate J* 1969;6:471–87. [PubMed: 5260755]
- Incardona JP, Roelink H. The role of cholesterol in Shh signaling and teratogen-induced holoprosencephaly. *Cell Mol Life Sci* 2000;57:1709–19. [PubMed: 11130177]
- Ingham PW, McMahon AP. Hedgehog signaling in animal development: paradigms and principles. *Genes Dev* 2001;15:3059–87. [PubMed: 11731473]
- Jeong J, Mao J, Tenzen T, Kottmann AH, McMahon AP. Hedgehog signaling in the neural crest cells regulates the patterning and growth of facial primordia. *Genes Dev* 2004;18:937–51. [PubMed: 15107405]
- Jiang R, Bush JO, Lidral AC. Development of the upper lip: Morphogenetic and molecular mechanisms. *Dev Dyn* 2006;235:1152–66. [PubMed: 16292776]
- Juriloff DM, Harris MJ. Mouse genetic models of cleft lip with or without cleft palate. *Birth Defects Res A Clin Mol Teratol* 2008;82:63–77. [PubMed: 18181213]
- Keeler RF. Cycloamine and related steroidal alkaloid teratogens: their occurrence, structural relationship, and biologic effects. *Lipids* 1978;13:708–15. [PubMed: 723484]
- Laron Z, Taube E, Kaplan I. Pituitary growth hormone insufficiency associated with cleft lip and palate. An embryonal developmental defect. *Helv Paediatr Acta* 1969;24:576–81. [PubMed: 5370797]
- Lauth M, Bergstrom A, Toftgard R. Phorbol esters inhibit the Hedgehog signalling pathway downstream of Suppressor of Fused, but upstream of Gli. *Oncogene* 2007;26:5163–8. [PubMed: 17310984]
- Leoncini E, Baranello G, Orioli IM, Anneren G, Bakker M, Bianchi F, Bower C, Canfield MA, Castilla EE, Cocchi G, Correa A, De Vigan C, Doray B, Feldkamp ML, Gatt M, Irgens LM, Lowry RB, Maraschini A, Mc Donnell R, Morgan M, Mutchinick O, Poetzsch S, Riley M, Ritvanen A, Gnansia ER, Scarano G, Sipek A, Tenconi R, Mastroiacovo P. Frequency of holoprosencephaly in the International Clearinghouse Birth Defects Surveillance Systems: searching for population variations. *Birth Defects Res A Clin Mol Teratol* 2008;82:585–91. [PubMed: 18566978]
- Li YX, Yang HT, Zdanowicz M, Sicklick JK, Qi Y, Camp TJ, Diehl AM. Fetal alcohol exposure impairs Hedgehog cholesterol modification and signaling. *Lab Invest* 2007;87:231–40. [PubMed: 17237799]
- Lipinski RJ, Dengler E, Kiehn M, Peterson RE, Bushman W. Identification and characterization of several dietary alkaloids as weak inhibitors of hedgehog signaling. *Toxicol Sci* 2007;100:456–63. [PubMed: 17728282]
- Lipinski RJ, Hutson PR, Hannam PW, Nydza RJ, Washington IM, Moore RW, Girdaukas GG, Peterson RE, Bushman W. Dose- and route-dependent teratogenicity, toxicity, and pharmacokinetic profiles of the hedgehog signaling antagonist cycloamine in the mouse. *Toxicol Sci* 2008a;104:189–97. [PubMed: 18411234]
- Lipinski RJ, Bushman W, Rowland IJ. MR investigation of a teratogen-mediated mouse model of cleft lip and palate. *Proc ISMRM* 2008b:2485.

- Maity T, Fuse N, Beachy PA. Molecular mechanisms of Sonic hedgehog mutant effects in holoprosencephaly. *Proc Natl Acad Sci U S A* 2005;102:17026–31. [PubMed: 16282375]
- Marcucio RS, Cordero DR, Hu D, Helms JA. Molecular interactions coordinating the development of the forebrain and face. *Dev Biol* 2005;284:48–61. [PubMed: 15979605]
- Matsunaga E, Shiota K. Holoprosencephaly in human embryos: epidemiologic studies of 150 cases. *Teratology* 1977;16:261–72. [PubMed: 594909]
- Murray JC. Gene/environment causes of cleft lip and/or palate. *Clin Genet* 2002;61:248–56. [PubMed: 12030886]
- Nanni L, Ming JE, Bocian M, Steinhaus K, Bianchi DW, Die-Smulders C, Giannotti A, Imaizumi K, Jones KL, Campo MD, Martin RA, Meinecke P, Pierpont ME, Robin NH, Young ID, Roessler E, Muenke M. The mutational spectrum of the sonic hedgehog gene in holoprosencephaly: SHH mutations cause a significant proportion of autosomal dominant holoprosencephaly. *Hum Mol Genet* 1999;8:2479–88. [PubMed: 10556296]
- Nopoulos P, Berg S, VanDemark D, Richman L, Canady J, Andreasen NC. Cognitive dysfunction in adult males with non-syndromic clefts of the lip and/or palate. *Neuropsychologia* 2002;40:2178–84. [PubMed: 12208013]
- Nopoulos P, Langbehn DR, Canady J, Magnotta V, Richman L. Abnormal brain structure in children with isolated clefts of the lip or palate. *Arch Pediatr Adolesc Med* 2007;161:753. [PubMed: 17679656]
- Parnell SE, O'Leary-Moore SK, Godin EA, Dehart DB, Johnson BW, Allan Johnson G, Styner MA, Sulik KK. Magnetic resonance microscopy defines ethanol-induced brain abnormalities in prenatal mice: effects of acute insult on gestational day 8. *Alcohol Clin Exp Res* 2009;33:1001–11. [PubMed: 19302087]
- Petiet AE, Kaufman MH, Goddeeris MM, Brandenburg J, Elmore SA, Johnson GA. High-resolution magnetic resonance histology of the embryonic and neonatal mouse: a 4D atlas and morphologic database. *Proc Natl Acad Sci U S A* 2008;105:12331–6. [PubMed: 18713865]
- Rice R, Connor E, Rice DP. Expression patterns of Hedgehog signalling pathway members during mouse palate development. *Gene Expr Patterns* 2006;6:206–12. [PubMed: 16168717]
- Richman RA, Sheehe PR, McCanty T, Vespasiano M, Post EM, Guzi S, Wright H. Olfactory deficits in boys with cleft palate. *Pediatrics* 1988;82:840–4. [PubMed: 3186373]
- Robin NH, Baty H, Franklin J, Guyton FC, Mann J, Woolley AL, Waite PD, Grant J. The multidisciplinary evaluation and management of cleft lip and palate. *South Med J* 2006;99:1111–20. [PubMed: 17100032]
- Roitman A, Laron Z. Hypothalamo-pituitary hormone insufficiency associated with cleft lip and palate. *Arch Dis Child* 1978;53:952–5. [PubMed: 747400]
- Rosset A, Spadola L, Ratib O. OsiriX: An Open-Source Software for Navigating in Multidimensional DICOM Images. *J Digit Imaging* 2004;17:205–216. [PubMed: 15534753]
- Rudman D, Davis T, Priest JH, Patterson JH, Kutner MH, Heymsfield SB, Bethel RA. Prevalence of growth hormone deficiency in children with cleft lip or palate. *J Pediatr* 1978;93:378–82. [PubMed: 211214]
- Schachter KA, Krauss RS. Murine models of holoprosencephaly. *Curr Top Dev Biol* 2008;84:139–70. [PubMed: 19186244]
- Schneider JE, Bose J, Bamforth SD, Gruber AD, Broadbent C, Clarke K, Neubauer S, Lengeling A, Bhattacharya S. Identification of cardiac malformations in mice lacking Ptdsr using a novel high-throughput magnetic resonance imaging technique. *BMC Dev Biol* 2004;4:16. [PubMed: 15615595]
- Smiley, GR.; Vanek, RJ.; Dixon, SD. Cleft Palate J. Vol. 8. 1971. Width of the craniofacial complex during formation of the secondary palate; p. 371-78.
- Subtelny JD. Width of the nasopharynx and related anatomic structures in normal and unoperated cleft palate children. *Am J Orthod* 1955;41:889–909.
- Sulik KK, Dehart DB, Rogers JM, Chernoff N. Teratogenicity of low doses of all-trans retinoic acid in presomite mouse embryos. *Teratology* 1995;51:398–403. [PubMed: 7502239]

- Sulik KK, Johnston MC. Sequence of developmental alterations following acute ethanol exposure in mice: craniofacial features of the fetal alcohol syndrome. *Am J Anat* 1983;166:257–69. [PubMed: 6846205]
- Swanenburg de Veye HF, Beemer FA, Mellenbergh GJ, Wolters WH, Heineman-de Boer JA. An investigation of the relationship between associated congenital malformations and the mental and psychomotor development of children with clefts. *Cleft Palate Craniofac J* 2003;40:297–303. [PubMed: 12733960]
- Taipale J, Cooper MK, Maiti T, Beachy PA. Patched acts catalytically to suppress the activity of Smoothened. *Nature* 2002;418:892–7. [PubMed: 12192414]
- Vieira AR. Unraveling human cleft lip and palate research. *J Dent Res* 2008;87:119–25. [PubMed: 18218836]
- Williams JA, Guicherit OM, Zaharian BI, Xu Y, Chai L, Wichterle H, Kon C, Gatchalian C, Porter JA, Rubin LL, Wang FY. Identification of a small molecule inhibitor of the hedgehog signaling pathway: effects on basal cell carcinoma-like lesions. *Proc Natl Acad Sci U S A* 2003;100:4616–21. [PubMed: 12679522]

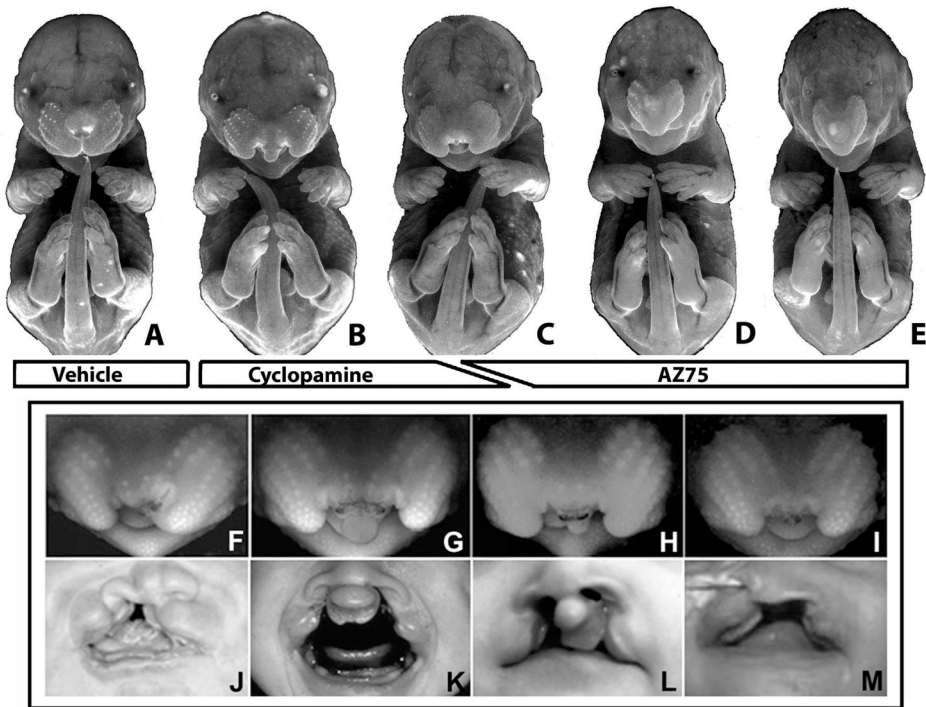


Figure 1. Hh signaling antagonist-induced CLP- and HPE- associated dysmorphology
 GD16.5 fetuses exposed to vehicle (A), cycloamine (B, F–H), or the cycloamine analog, AZ75 (C–E). Cycloamine exposure induced unilateral and bilateral CLP (B). AZ75 exposure predominantly induced severe holoprosencephalic phenotypes within the range shown in D and E. An intermediate CLP phenotype presenting with severely deficient medial nasal prominence derived tissue (C, I) was induced infrequently by both drug administration regimens. The phenotypic range produced by cycloamine exposure included unilateral CLP (F), bilateral CLP with graded amounts of medial nasal prominence derived tissue (G,H), and median CL with cleft palate (I). Correlate human phenotypes are shown below. Images are presented courtesy of M. Muenke (J,L,M) and K. Sulik (K).

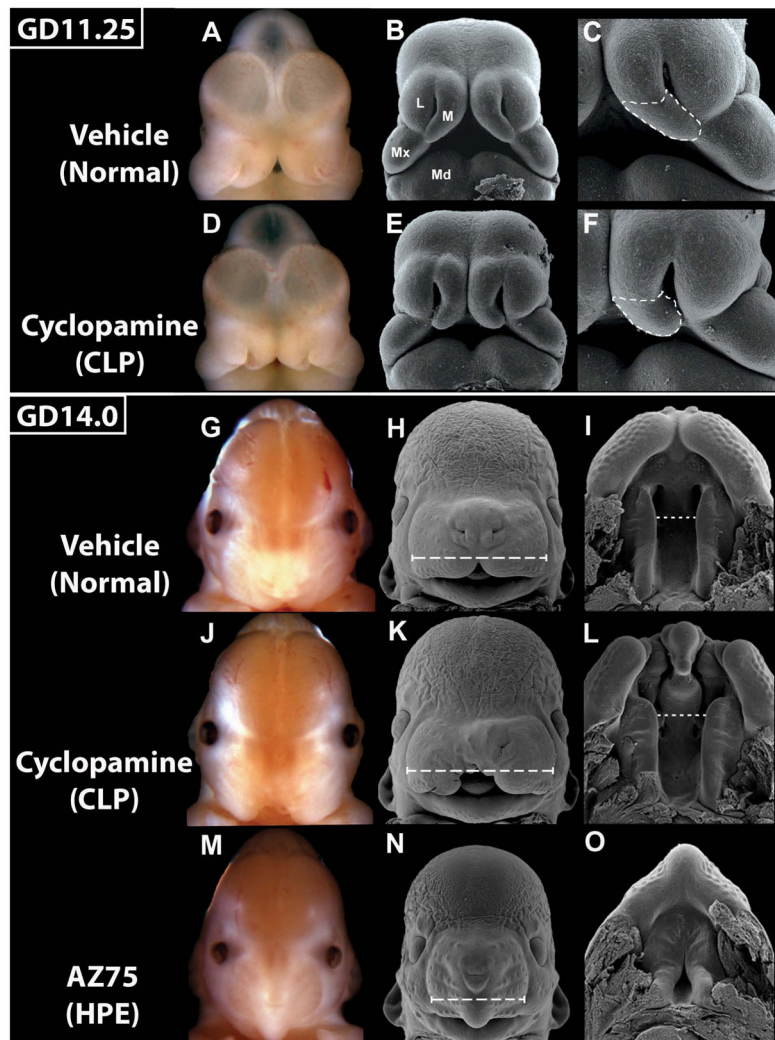


Figure 2. Embryonic morphogenesis of cyclopamine-induced CLP

Bright field and scanning electron microscopy images of GD11.25 and 14.0 embryos exposed to vehicle, cyclopamine, or AZ75. At GD11.25, the medial nasal (M), lateral nasal (L), and maxillary (Mx) prominences have united in normal embryos (A–C) to form the upper lip. In affected cyclopamine-exposed embryos (D–F), the medial nasal prominences are too closely opposed at the juncture between the upper and lower aspects, with the lower aspect (dashed outline) deficient in size and angle relative to normal. At GD14.5, in normal embryos (G–I), the maxillary-derived secondary palatal shelves have fused with the primary palate and begun to elevate (I). Cyclopamine-exposed embryos with unilateral CL (K) and bilateral CL (L), exhibit excessive midface width (long dashed lines) and palatal shelves that appear normal in size and conformation but are too widely spaced (short dashed lines) in the anterior aspect. In AZ75-exposed cebocephalic embryos (M–O), the primary palate is absent and secondary palatal shelves have prematurely fused anteriorly. Mandibular prominence (Md).

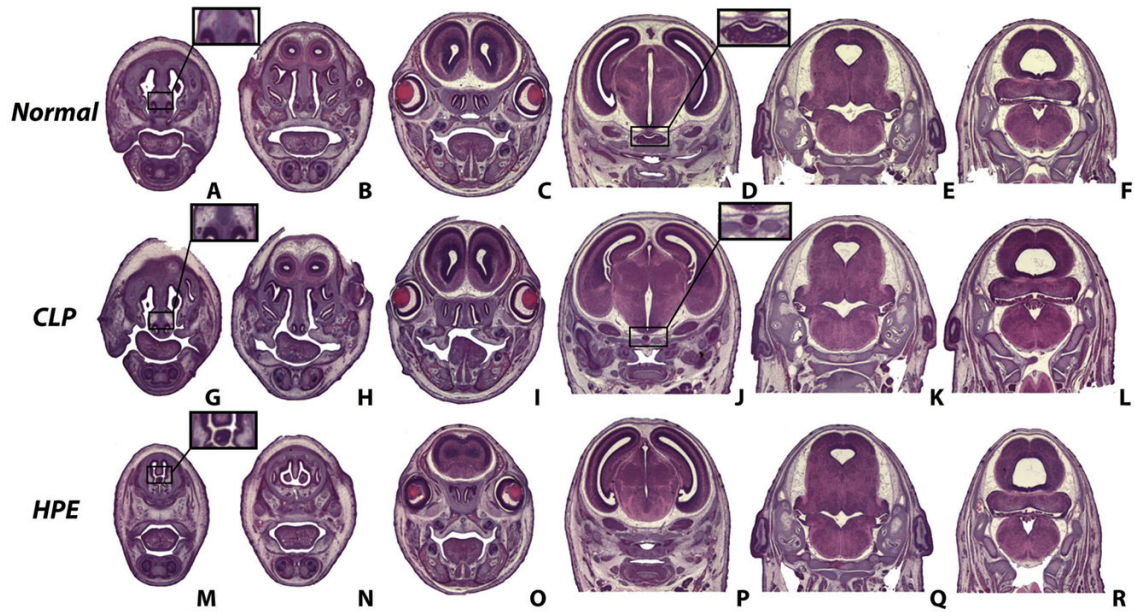


Figure 3. Histological analysis of CLP- and HPE-associated craniofacial and CNS phenotype
 Hematoxylin and eosin-stained serial coronal sections of GD 16.5 fetuses exposed to vehicle (A–F), cyclopamine (G–L), or AZ75 (M–R). Notable CLP-associated features include small secondary palate shelves (I) and anterior pituitary gland agenesis (J). Notable HPE-associated features include absent nasal septum cartilage (M), olfactory bulb agenesis (N), rostral union of the cerebral hemispheres with fused striatum (O), and complete pituitary gland agenesis (P). Sections D and J were chosen because they feature the most prominent pituitary gland mass. No apparent differences in midbrain and hindbrain features were noted.

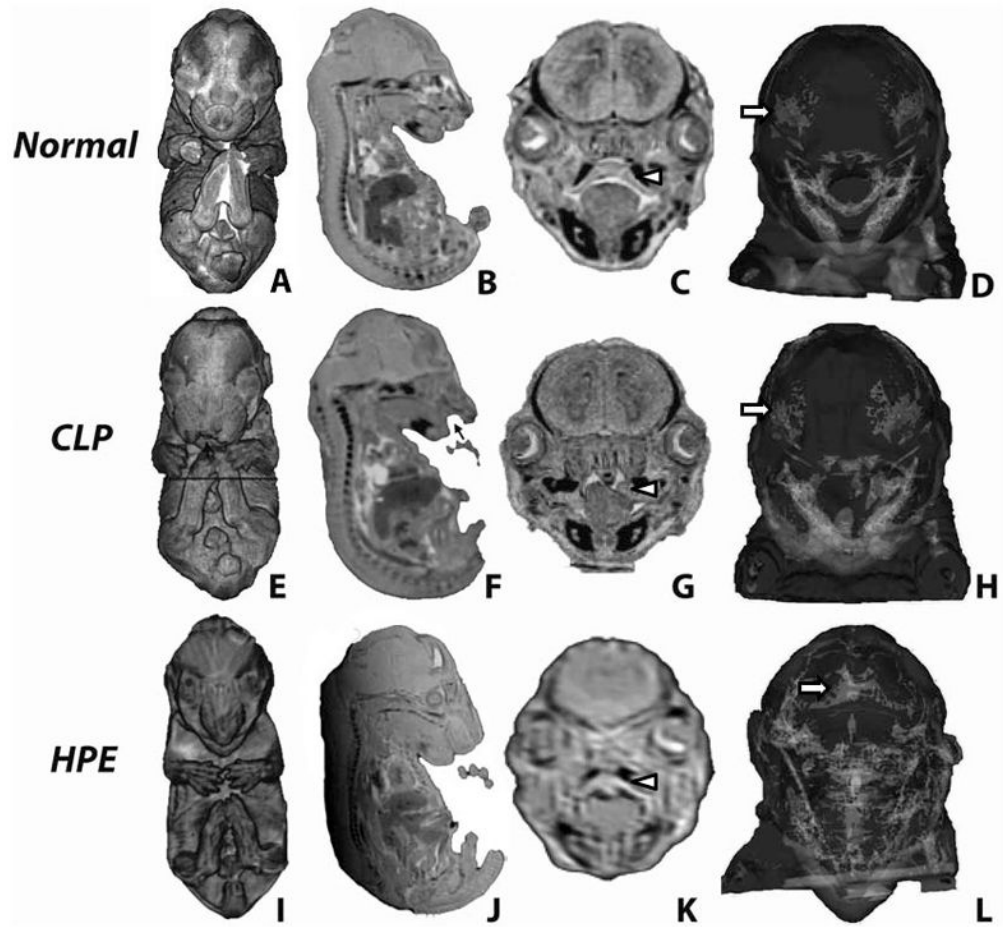


Figure 4. MRI-based fetal phenotypic analysis

3-D volume (A,E,I) and surface rendering (D,H,L) and 2D sections (B,C,F,G,J,K) reveal external and internal CLP- and HPE-associated dysmorphology. Cleft lip is indicated by black arrows while white arrowheads note secondary palate structure. White arrows note cranial frontal bones which are abnormally fused (metopic craniosynostosis) in the HPE fetus (L).

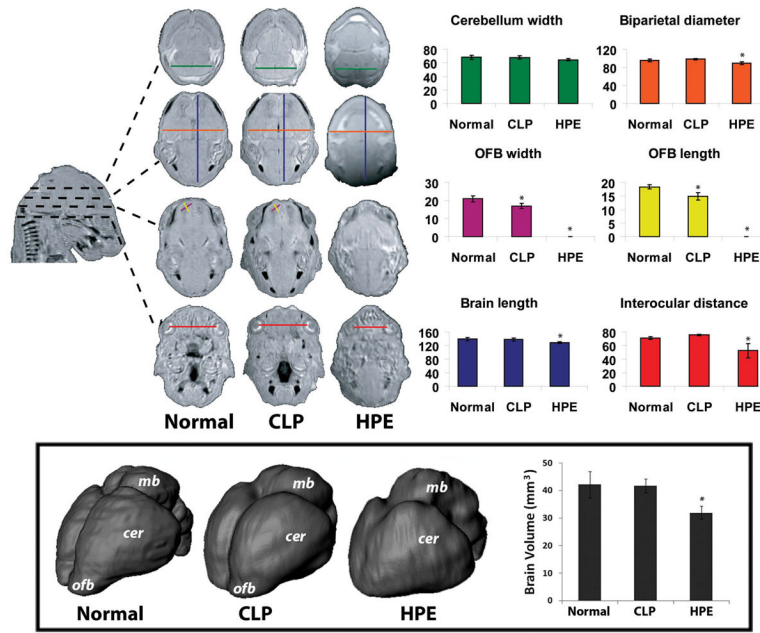


Figure 5. HPE and CLP associated CNS phenotype

Linear measurements (arbitrary units) were produced from serial transverse sections. Olfactory bulb (OFB) length and width were reduced in the CLP group. In the HPE group, biparietal diameter, brain length, and interocular distance were reduced and olfactory bulbs were absent. 3-D whole brain reconstructions were produced from MRI data (boxed). ofb – olfactory bulb; cer – cerebral hemisphere; mb – midbrain. Plot shows corresponding quantitation of total brain volume. A subtle but consistent hypoplasia of the olfactory bulbs was found in the CLP group. In the HPE group, median union and rostro-caudal foreshortening of the cerebral hemispheres was found along with a gross reduction in brain volume.